atmosphere

MDPI

Article

Aqueous Reactions of Sulfate Radical-Anions with Nitrophenols in Atmospheric Context

Krzysztof J. Rudziński * and Rafał Szmigielski

Institute of Physical Chemistry of the PAS, Kasprzaka 44/52, 01-224 Warsaw, Poland; rafal.szmigielski@gmail.com

* Correspondence: kjrudz@ichf.edu.pl; Tel.: +48-22-343-3402

Received: 14 November 2019; Accepted: 4 December 2019; Published: 9 December 2019

Abstract: Nitrophenols, hazardous environmental pollutants, react promptly with atmospheric oxidants such as hydroxyl or nitrate radicals. This work aimed to estimate how fast nitrophenols are removed from the atmosphere by the aqueous-phase reactions with sulfate radical-anions. The reversed-rates method was applied to determine the relative rate constants for reactions of 2-nitrophenol, 3-nitrophenol, 4-nitrophenol, 2,4-dinitrophenol, and 2,4,6-trinitrophenol with sulfate radical-anions generated by the autoxidation of sodium sulfite catalyzed by iron(III) cations at ~298 K. The constants determined were: 9.08×10^8, 1.72×10^9, 6.60×10^8, 2.86×10^8, and 7.10×10^7 M^{-1} s^{-1}, respectively. These values correlated linearly with the sums of Brown substituent coefficients and with the relative strength of the O–H bond of the respective nitrophenols. Rough estimation showed that the gas-phase reactions of 2-nitrophenol with hydroxyl or nitrate radicals dominated over the aqueous-phase reaction with sulfate radical-anions in deliquescent aerosol and haze water. In clouds, rains, and haze water, the aqueous-phase reaction of 2-nitrophenol with sulfate radical-anions dominated, provided the concentration of the radical-anions was not smaller than that of the hydroxyl or nitrate radicals. The results presented may be also interesting for designers of advanced oxidation processes for the removal of nitrophenol.

Keywords: atmospheric processes; secondary organic aerosol; rate constants; atmospheric pollutants; advanced oxidation processes

1. Introduction

Nitrophenols are well known environmental trace compounds and pollutants [1,2], which have been detected in various environmental matrices including air [3–6], rainwater [3,7–9], cloud water [10], fog [10,11], snow [1], atmospheric aerosol [4–6,12–25], soils [26,27], and surface waters [10,28–32]. They originate from many anthropogenic and natural sources including: the incineration of wastes [33], industrial chemical processes [34], combustion of coal and biomass as well as vehicle and aviation fuels [35–37], degradation of pesticides [34,38,39], release of wood preservatives [34], and atmospheric chemical reactions. 4-nitrophenol (4-NP) and 2,4-dinitrophenol (2,4-DNP), along with sugar anhydrides such as levoglucosan, serve as markers of biomass burning in ambient aerosol [40–43]. These compounds and 2-nitrophenol are recognized components of atmospheric brown carbon, i.e., a collection of light absorbing organic compounds in the atmosphere [22,44,45]

Atmospheric reactions that yield nitrophenols take place both in the gas phase and in the aqueous phase. For instance, the gas-phase nitration of phenol involves hydroxyl radicals $^{\bullet}OH$ and NO_2 in the daytime or nitrate radical $^{\bullet}NO_3$ and NO_2 in the night to respectively produce 2-nitrophenol (2-NP) or 2-NP and 4-NP. The chemical mechanisms of both processes were thoroughly reviewed [1]. Formation of nitrophenols in atmospheric waters of all kinds is at least equally important but less understood. The possible pathways include oxidation of phenols with NO_2 and OH or NO_3 radicals [46], electrophilic nitration initiated by N_2O_5 and $ClNO_2$ [1,47], photolytic and dark reactions involving nitrate radicals, inorganic nitrates, nitrites and nitrous acid HONO [48,49], and photolytic reactions with nitrogen dioxide in the presence of iron oxide and oxygen [49].

Atmospheric sinks for nitrophenols include photolysis [50] and the gas-phase reactions with OH radicals and NO_3 radicals [51,52] which are characterized by the estimated residence time of several days. More efficient sinks may include partitioning to atmospheric aqueous phases followed by reactions with various radicals and/or photolysis [1,46]. More recently, Barsotti, et al. [53] demonstrated that the irradiation of aqueous solutions or viscous films containing several nitrophenols (2-NP, 4-NP, 2,4-DNP, and 2,6-DNP, i.e., 2,6-dinitrophenol) was an efficient source of HONO and NO_2^- ions. Vione, et al. [54] showed that OH radicals reacted faster than NO_3 radicals with 2-NP and 4-NP in aqueous solutions to lower the atmospheric levels of 2-NP below those of 4-NP. Hems and Abbatt [55] studied the aqueous-phase photo-oxidation of 2,4-DNP by OH radicals, identified numerous intermediate products thereof and showed the corresponding evolution of UV absorbance of the reacting solutions. In addition, many laboratories studied the aqueous-phase reactions of other substituted phenols of atmospheric interest like guaiacol, nitro-guaiacol, vanillin, or syringol [55–59].

Much of the nitrophenol chemistry has been studied for the sake of advanced oxidation processes aimed at mitigation of nitrophenols in aquatic and industrial environments [60]. The technologies considered include: Fenton and photo-Fenton reactions based on H_2O_2 [34,61], TiO_2 based photocatalysis [62–64], electrocatalysis [65], photo-electrocatalysis [66,67], and wet catalysis [68,69]. Among the latter, a promising process was proposed which utilized reactions of nitrophenols with sulfate radical-anions generated by the cobalt-mediated decomposition of peroxymonosulfate anions [70].

For years, some nitrophenols (2-NP, 4-NP, 2,4-DNP) have been listed as priority or hazardous pollutants [71–73]. Generally, mono- and di-nitrophenols are considered toxic in plants and mammals [74], while 4-nitrophenol is highly toxic in humans [75]. Although EPA USA has not considered 4-nitrophenol carcinogenic [38], a laboratory experiment showed the compound can destroy DNA in vitro [76].

This work was aimed at elucidating how fast nitrophenols are removed from the atmospheric waters by reaction with sulfate radical-anions, which are important atmospheric oxidants known to react fast with numerous atmospheric pollutants [77–83].

2. Experiments

2.1. Chemicals

The following chemicals were used as purchased: 2-nitrophenol (R.G.), 3-nitrophenol (REAGENTPLUS™, 99%), 4-nitrophenol and 2,4,6-trinitrophenol (1 wt % solution in water) from Sigma Aldrich, 2,4-dinitrophenol (97% + 15% H_2O) from Alfa Aesar, $Fe(ClO_4)_3 \cdot 9H_2O$ (purum) from Fluka, $Na_2S_2O_5$ (EMSURE® ACS, Reag. Ph Eur. > 98%) and $HClO_4$ (pro analysis) from Merck, argon (99.999%) from Multax. For each experiment, aqueous solutions of reactants were prepared freshly using Milli-Q water (18.2 MΩ cm, Milli-Q Advantage System from Merck Millipore). Buffer standards used for the calibration of pH electrodes were from Thermo Fisher Scientific. To avoid the contact with the atmospheric oxygen, Milli-Q water was deoxygenated by a stream of argon bubbled through for 20 min. Solutions of sodium bisulfite were obtained by dissolving $Na_2S_2O_5$ in deoxygenated Milli-Q water

$$Na_2S_2O_5 + H_2O \rightleftarrows 2Na^+ + 2HSO_3^-, \tag{1}$$

The acidity of solutions was adjusted to pH = 3.1 with 0.1 M $HClO_4$ so the species in solutions were predominantly Na^+ and HSO_3^- ions.

2.2. Estimation of the Rate Constants

The relative rate constants for reactions of nitrophenols with sulfate radical-anions were estimated using the reversed-rates method developed by Ziajka and Pasiuk-Bronikowska [84] and successfully applied to several organic compounds [83,85,86]. Briefly, the sulfate radical-anions are generated during chain autoxidation of sulfite anions catalyzed by Fe(III) cations. The mechanism of the autoxidation was presented in detail by Ziajka and Rudziński [83] and recalled in the SI. One runs several experiments with the autoxidation of S(IV) inhibited by two different compounds, inh1 and inh2, used at several different initial concentrations (e.g., Figure 1). Each experiment should attain a pseudo-stationary phase during which the autoxidation proceeds at a constant rate (e.g., Figure 2). Then, one plots the reciprocal stationary rates observed against the initial concentrations of the inhibitor used (Figure 3). If both plots are linear, the ratio of rate constants for reactions of the inhibitors with sulfate radical-anions is equal to the ratio of the slopes of the linear plots (Equation (2)). If one knows the rate constant for reaction of one inhibitor with sulfate radical-anions, one can calculate the rate constant for the other inhibitor.

$$k_{\mathrm{inh1+SO_4^-}} = \frac{\mathrm{slope_{inh1}}}{\mathrm{slope_{inh2}}} k_{\mathrm{inh2+SO_4^-}}, \tag{2}$$

In the present work, ethanol was used as a reference inhibitor against which the rate constants for nitrophenols were calculated.

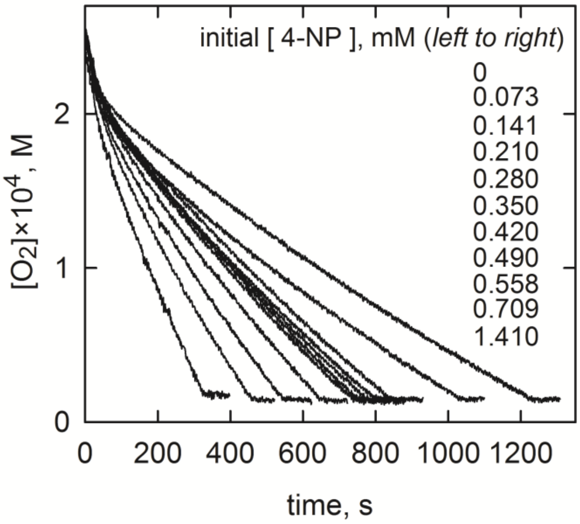

Figure 1. Concentration of oxygen recorded during autoxidation of $NaHSO_3$ inhibited by 4-NP at various initial concentrations.

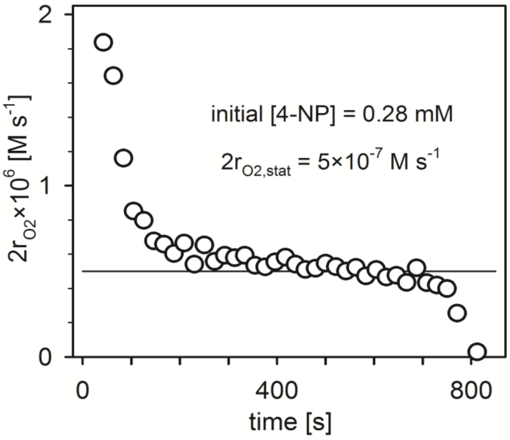

Figure 2. Rate of oxygen consumption during autoxidation of $NaHSO_3$ inhibited by 4-NP (initially 0.28 mM) evaluated from data in Figure 1.

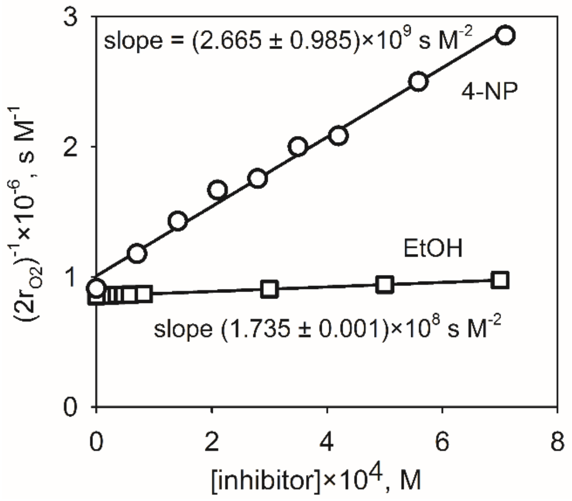

Figure 3. Linear plots of reciprocal quasi-stationary rates of the autoxidation of $NaHSO_3$ inhibited by 4-NP or by the reference ethanol versus initial concentrations of each inhibitor. The slope uncertainties are equal to standard errors of regression coefficients.

2.3. Experimental Runs

The experimental setup and procedure for carrying out the stationary autoxidation of S(VI) inhibited by organic compounds was described in detail elsewhere [83]. Briefly, the experiments were carried out in a well-mixed glass reactor of 60 cm^3 volume, closed with a Teflon cover and thermostatted at 298 K within a water jacket. For each run, the reactor was filled with aqueous solution of sodium bisulfite and oxygen so that it contained no gas phase. The pH of solution was adjusted to 3.1 with $HClO_4$. The pH of the solution was recorded using a SenTix Mic combination pH electrode from WTW. Then, a small aliquot of aqueous solution of $Fe(ClO_4)_3$ catalyst was injected to start the reaction. Table 1 shows the initial concentrations of reactants. The autoxidation of S(IV) was followed by recording the concentration of oxygen using an Orion 97-08 from Thermo Fisher Scientific and a home-designed pH/oxygen meter and software. Equation (3a) shows the overall stoichiometry of uninhibited SIV autoxidation. Assuming the conversion of inhibitors was small, the stoichiometry of the autoxidation inhibited by a nitrophenol was defined by the same equation so that the rate of the autoxidation was defined by Equation (3b) [83].

$$2SO_3^{2-}/2HSO_3^- + O_2 = SO_4^{2-}/HSO_4^-, \tag{3a}$$

$$r_{autoxidation} = -\frac{d[S(IV)]}{dt} = \frac{d[S(VI)]}{dt} = -2\frac{d[O_2]}{dt}, \tag{3b}$$

Table 1. Initial concentrations of reactants used in the experiments.

Compound	Abbreviation	Concentration Range, mM
2-nitrophenol	2-NP	0.032–0.347
3-nitrophenol	3-NP	0.019–0.089
4-nitrophenol	4-NP	0.073–0.711
2,4-dinitrophenol	2,4-DNP	0.169–1.325
2,4,6-trinitrophenol	2,4,6-TNP	0.197–0.788
HSO_3^-		2
O_2		~0.25
$Fe(ClO_4)_3$		0.01

2.4. Correction of the Diffusional Limitations of the Rate Constants

Since the reactions examined were very fast, we corrected the rate constants determined for diffusional limitations using a simple resistance-in-series model [87–90]

$$k_{observed}^{-1} = k_{reaction}^{-1} + k_{diffusion}^{-1}, \tag{4}$$

$$k_{diffusion} = 4\pi(D_A + D_B)(r_A + r_B)N \times 10^3, \tag{5}$$

where all k are second order rate constants (M^{-1} s^{-1}), D are diffusion coefficients of reactants A and B (m^2 s^{-1}), r are reaction radii of reactant molecules A and B (m), and N is the Avogadro number (mol^{-1}). Details of the calculations are summarized in Section S3 of the SI.

3. Results

In this section, we present the experimental results obtained for 4-NP. The results for other nitrophenols were similar so we present them in the SI. Figure 1 shows consumption of oxygen during the autoxidation of S(IV) in the presence of 4-NP. The higher was the initial concentration of nitrophenol, the slower was the consumption of O_2.

In each experiment, the autoxidation attained a quasi-stationary rate, as shown in Figure 2 for the run with [4-NP] = 0.28 mM.

Figure 3 shows the plots of reciprocal stationary rates for autoxidation of S(IV) in the presence of 4-NP or a reference compound ethanol versus initial concentrations of each inhibitor. The plots were linear, so their slopes were used in Equation (2) to calculate the relative rate constant for the reaction of 4-NP with sulfate radical-anions

$$k_{4\text{-NP}+SO_4^-} = k_{\text{EtOH}+SO_4^-} \frac{\text{slope}_{4\text{-NP}}}{\text{slope}_{\text{EtOH}}} = 4.3 \times 10^7 \frac{2.665 \times 10^9}{1.735 \times 10^8} = 6.636 \times 10^8 \ \text{M}^{-1}\text{s}^{-1}, \tag{6}$$

Plots for other nitrophenols, all of them linear, were placed in the SI. The results of all experiments are collected in Table 2 and include the slopes of linear plots and the rate constants for reactions of nitrophenols with sulfate radical-anions, both observed and corrected for diffusional limitations. The uncertainties of the observed rate constants were estimated using the total differential method applied to Equation (6) with individual errors equal to the standard errors of the linear slopes and k_{EtOH} (Table 2). The uncertainties of the corrected rate constants were estimated in a similar way from Equation (4), assuming arbitrarily the uncertainty of $k_{difffusion}$ was 10%.

Table 2. Experimental slopes of linear plots (Figure 3 and Figure S2) and rate constants for reactions of nitrophenols with sulfate radical-anions (observed and corrected for diffusional limitations).

Compound	Slope, s M^{-2}	$k_{observed}$, $M^{-1}s^{-1}$	$k_{diffusion}{}^{A}$, $M^{-1}s^{-1}$	$k_{reaction}$, $M^{-1}s^{-1}$	$(k_r - k_o)/k_o$, %
EtOH (*reference*)	$(1.735 \pm 0.001) \times 10^8$			$(4.30 \pm 0.86) \times 10^7$	
2-NP	$(3.662 \pm 0.235) \times 10^9$	$(9.08 \pm 2.40) \times 10^8$	2.01×10^{10}	$(9.50 \pm 4.58) \times 10^8$	4.74
3-NP	$(6.957 \pm 0.277) \times 10^9$	$(1.72 \pm 0.41) \times 10^9$	2.01×10^{10}	$(1.89 \pm 0{,}89) \times 10^9$	9.53
4-NP	$(2.665 \pm 0.985) \times 10^9$	$(6.60 \pm 3.77) \times 10^8$	2.01×10^{10}	$(6.83 \pm 5.42) \times 10^8$	3.41
2,4-DNP	$(1.154 \pm 0.152) \times 10^9$	$(2.86 \pm 0.95) \times 10^8$	2.13×10^{10}	$(2.90 \pm 1.58) \times 10^8$	1.51
2,4,6-TNP	$(2.865 \pm 0.180) \times 10^8$	$(7.10 \pm 1.87) \times 10^7$	2.18×10^{10}	$(7.12 \pm 3.31) \times 10^7$	0.33

A—assumed uceratinty 2×10^9 M^{-1} s^{-1}(10%).

4. Discussion

4.1. Hammett's Correlations

The reactions of nitrophenols with sulfate radical-anions appeared quite fast, with observed second order rate constants of the order 10^9 s^{-1} M^{-1} (Table 2). However, the diffusional limitations were not significant because the rate constants corrected for diffusional limitations were higher for a few percent only. The rate constants decreased with the number of NO_2 groups in the molecule with the exception of 3-NP. Figure 4a shows the uncorrected rate constants for reactions of sulfate radical-anions with phenol and substituted phenols—chlorophenols [83] and nitrophenols (this work)—correlate well with sums of Brown substituent coefficients for the compounds. The Brown coefficients for chlorophenols were taken after [83], while those for nitrophenols were: $\sigma_m{}^+ = 0.71$, $\sigma_p{}^+ = 0.79$ [91,92] and $\sigma_o{}^+ = 0.66$ $\sigma_p{}^+ = 0.52$ [93] for *meta*, *para* and *orto* substituents, respectively. The straight line in Figure 4a was obtained by linear regression covering all data (Equation (7)).

$$\log\left(k_{SO_4}\right) = (9.9006 \pm 0.0785) - (1.1513 \pm 0.0970)\sum \sigma^+, \quad R^2 = 0.9663, \tag{7}$$

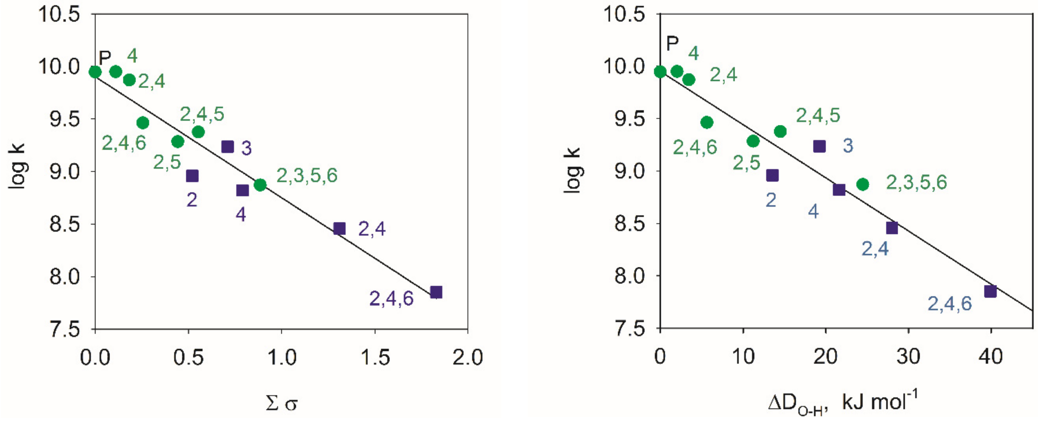

(**a**) (**b**)

Figure 4. Correlation of rate constants for reactions of sulfate radical-anions with phenol (P), chlorophenols (green circles: 4-CP; 2,4-DCP; 2,5-DCP; 2,4,5-TCP; 2,4,6-TCP; 2,3,5,6-TTCP) [83] and nitrophenols (blue squares: 2-NP; 3-NP; 4-NP; 2,4-DNP; 2,4,6-TNP) [this work] against (**a**) sums of Brown substituent coefficients and (**b**) the relative strength of the O–H bond.

Equation (7) can be used to estimate the second order rate constants for reactions of sulfate radical-anions with substituted phenols that had not been determined experimentally.

The Brown substituent coefficients can estimate the relative strength of the O–H bonds in substituted phenols with a linear correlation developed by Jonsson et al. [93] (Equation (8)).

$$\Delta D_{O\text{–}H} = -2 + 29.9\left(\sigma^+_{o2} + \sigma^+_{m3} + \sigma^+_{p4} + \sigma^+_{m5} + \sigma^+_{o6}\right), \quad \text{kJ mol}^{-1}, \tag{8}$$

Therefore, the rate constants for reactions of sulfate radical-anions with phenol and substituted phenols can also be correlated against $\Delta D_{O\text{–}H}$ (Figure 4b). The corresponding linear regression is given by Equation (9).

$$\log\left(k_{SO_4}\right) = (9.9498 \pm 0.0828) - (0.0508 \pm 0.0043)\Delta D_{O\text{–}H}, \quad R^2 = 0.9665, \tag{9}$$

Equation (9) can estimate the second order rate constants for reactions of sulfate radical-anions with substituted phenols in place of Equation (7).

4.2. Atmospheric Significance

The atmospheric significance of the aqueous-phase reactions of nitrophenols with sulfate radical-anions was evaluated using the approach developed in [81]. The rate of the total conversion of a nitrophenol NP by a reactant X (OH or NO_3) in the gas phase ($r_{X,g}$) and in the aqueous phase ($r_{X,aq} \times \omega$) was compared to the rate of conversion of this NP by sulfate radical-anions in the aqueous phase within the gas phase ($r_{SO_4,aq}\ \omega$) as the ratio $R_{X,tot\text{-}aq}$ defined by Equation (10). The concentrations of the gas-phase and aqueous-phase reactants were assumed to follow the Henry's Law.

$$R_{X,tot-aq} = \frac{r_{X,g} + r_{X,aq}\omega}{r_{SO_4,aq}\omega} = \frac{k_{X,g}[X]_g[NP]_g + k_{X,aq}[X]_{aq}[NP]_{aq}\omega}{k_{SO_4,aq}[X]_{aq}\left[SO_4^{\cdot-}\right]_{aq}\omega} = \frac{\frac{k_{X,g}}{H_{d,X}H_{d,NP}} + k_{X,aq}\omega}{k_{SO_4,aq}\omega} \cdot \frac{[X]_{aq}}{\left[SO_4^{\cdot-}\right]_{aq}}, \quad (10)$$

where ω m^3 m^{-3} is the atmospheric liquid water contents; $k_{X,g}$ and $k_{X,aq}$ dm^3 mol^{-1} s^{-1} are the rate constant for the reaction of X with NP in the gas phase and the aqueous phase, respectively; $k_{SO_4,aq}$ dm^3 mol^{-1} s^{-1} is the rate constant for the reaction of $SO_4^{\bullet-}$ with NP in the aqueous phase; H_d is the dimensionless Henry's constant ($H_d = H \times$ gas constant $\times$ absolute temperature) for X or for NP; $[X]_{aq}$ and $[SO_4^{\bullet-}]_{aq}$ are the aqueous-phase concentrations of X and $SO_4^{\bullet-}$.

Figure 5 compares the total conversion of 2-NP due to the gas-phase and the aqueous-phase reactions with OH radicals to the aqueous-phase reaction with $SO_4^{\bullet-}$ radical-anions (a) as well as the conversion of 2-NP due to the gas-phase and aqueous-phase reactions with NO_3 radicals to the aqueous-phase reaction with $SO_4^{\bullet-}$ radical-anions (b). Data required for the calculations behind the plots are given in Tables 2 and 3 while more details are available in the SI. The ranges of radical concentrations considered in Figure 5 fit well within the realistic ranges estimated by modeling for the atmospheric systems (Table 4) [94].

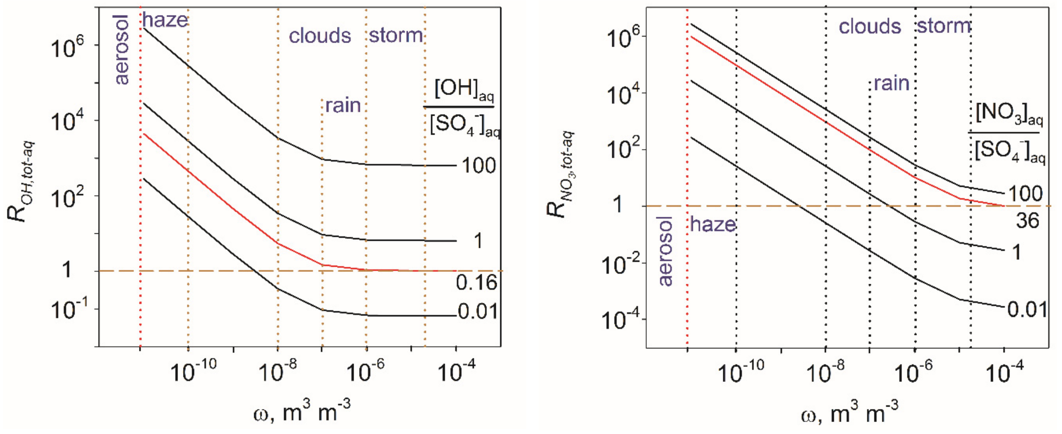

(**a**) (**b**)

Figure 5. Total rate of 2-NP conversion in the atmosphere due the gas-phase and aqueous-phase reactions with OH radicals (**a**) or NO_3 radicals (**b**) compared to the rate of the aqueous-phase reaction of 2-NP with sulfate radical-anions for various ratios of radicals in the aqueous phases ($[OH]_{aq}/[SO_4^{\bullet-}]_{aq}$) and various liquid water contents ω (based on Equation (10)).

In most cases, the total OH radical sink for 2-NP dominates over the $SO_4^{\bullet-}$ aqueous sink in all atmospheric aqueous phases. Sulfate radical-anions take the lead only if they are in significant excess in clouds, rains, and storms (red line in Figure 5a, $[OH]_{aq}/[SO_4^{\bullet-}]_{aq} < 0.16$). The total NO_3 radical sink for 2-NP dominates over the $SO_4^{\bullet-}$ aqueous sink in aerosol and haze waters and in clouds and rains if in significant excess (red line in Figure 5b, $[NO_3]_{aq}/[SO_4^{\bullet-}]_{aq} > 36$). In other cases, the $SO_4^{\bullet-}$ aqueous sink prevails. The above rationale is based on the assumption that the hydroxyl and nitrate radicals as well as 2-NP are at Henry's equilibria in the gas phase and in the aqueous phase while the sulfate radical-anions exist only in the aqueous phase.

Table 3. Rate and Henry's constants for selected atmospheric reactants at 296–298 K.

Reaction X + NP	$k_{X,g}$		$k_{X,aq}$	H_{dX}	H_{dNP}
	cm^3 molecule^{-1} s^{-1}	**dm^3 mol^{-1} s^{-1}**	**dm^3 mol^{-1} s^{-1}**		
OH + 2-NP	9.00×10^{-13} (a)	5.42×10^8	5.90×10^9 (b)	6.11×10^2 (d)	5.17×10^3 (e)
NO_3 + 2-NP	2.00×10^{-14} (a)	1.20×10^7	2.30×10^7 (c)	1.47×10^1 (d)	

(a) [52,95]; (b) [54]; (c) [96]; (d) [81]; (e) [97].

Table 4. Ranges of radical concentrations in gas phase, clouds and deliquescent particles [94].

	Gas Phase [(a)]		Aqueous Phase				
	OH	**NO_3**	**OH**	**NO_3**	**$SO_4^{\bullet-}$**	**$[OH]/[SO_4^{\bullet-}]$**	**$[NO_3]/[SO_4^{\bullet-}]$**
	molecule cm^{-3}		**mol dm^{-3}**				
Minimal	1.4×10^{2}	7.9×10^{6}	1.4×10^{-16}	1.6×10^{-16}	5×10^{-17}	1.6×10^{-4}	1.8×10^{-3}
Maximal	6.6×10^{3}	1.2×10^{7}	8.0×10^{-12}	3.0×10^{-13}	9×10^{-13}	1.6×10^{5}	6.0×10^{3}

[(a)] calculated using Henry's constants from Table 3.

The rate of aqueous-phase reaction of a nitrophenol NP with sulfate radical-anions can also be compared to the rates of gas-phase reactions with OH or NO_3 sinks alone, assuming the gas-phase and aqueous-phase reactants follow the Henry's Law

$$R_{X,g-aq} = \frac{r_{X,g}}{r_{SO_4,aq}\omega} = \frac{k_{X,g}[X]_g[NP]_g}{k_{SO4,aq}[NP]_{aq}\left[SO_4^{\cdot -}\right]_{aq}\omega} = \frac{k_{X,g}}{k_{SO_4,aq}H_{d,\mathrm{X}}H_{d,\mathrm{NP}}\omega}\cdot\frac{[X]_{aq}}{\left[SO_4^{\cdot -}\right]_{aq}}, \tag{11}$$

The results obtained for 2-NP (Figure 6) show that the gas-phase sinks dominate in the aerosol and haze waters and in clouds and rains provided hydroxyl or nitrate radicals are in excess. Surprisingly, there is little difference observed between the hydroxyl radicals and nitrate radicals in spite of significant difference between the rate constants for their gas-phase reactions with 2-NP (Table 2). This is explained by lower solubility of NO_3 in water. When the aqueous-phase concentrations of both radicals are equal, the gas-phase concentration of NO_3 is higher than the concentration of OH and compensates for its lower rate constant. For reference, one can compare the gas-phase and the aqueous phase conversions of 2-NP by hydroxyl radicals or nitrite radicals alone (Figure S3). Conversion by OH in the gas phase dominates in over conversion in aerosol and haze water but not over that in clouds and rain. Conversion of 2-NP by NO_3 in the gas phase always dominates over conversion in atmospheric waters.

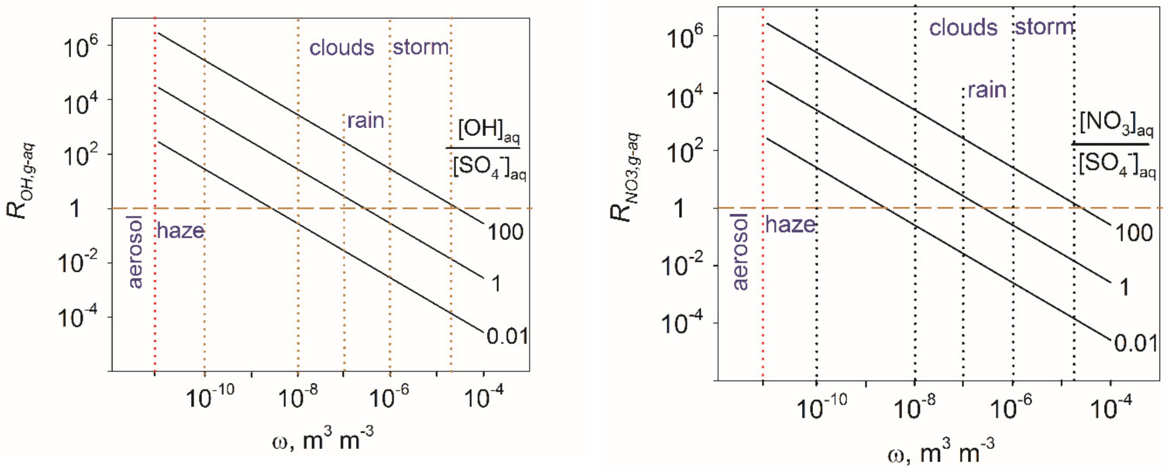

(**a**) (**b**)

Figure 6. Rate of 2-NP conversion in the atmosphere due to the gas-phase reaction with OH radicals (**a**) or with NO_3 radicals (**b**) compared to the rate of the aqueous-phase reaction of 2-NP with sulfate radical-anions for various proportions of radicals in the aqueous phase $[OH]_{aq}/[SO_4^{\bullet-}]_{aq}$ and varying liquid water contents (ω) (based on Equation (11)).

Rate of conversions of a NP by X (OH or NO_3) and by $SO_4^{\bullet-}$ in the aqueous phases alone were compared using Equation (12).

$$\frac{r_{\mathrm{X},aq}}{r_{\mathrm{SO_4},aq}} = \frac{k_{\mathrm{X},aq}}{k_{\mathrm{SO_4},aq}}\cdot\frac{[\mathrm{X}]_{aq}}{\left[\mathrm{SO}_4^{\cdot -}\right]_{aq}}, \tag{12}$$

Figure 7 shows that the aqueous-phase conversion of 2-NP by OH radicals dominates over that by $SO_4^{\bullet-}$ radical-anions when the ratio of the radicals concentrations is higher than ~0.15. A similar domination of NO_3 radicals over $SO_4^{\bullet-}$ radical-anions requires the corresponding concentration ratio is greater than ~40.

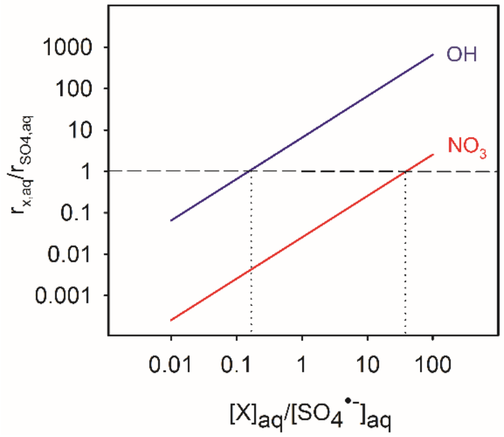

Figure 7. Comparison of the rates of aqueous-phase conversion of 2-NP due to reaction with $SO_4^{\bullet-}$ radicals and OH radicals (blue line) or NO_3 radicals (red line).

We expect the comparison of gas-phase and aqueous-phase conversions for other nitrophenols studied would provide similar results when the gas-phase rate constants for these nitrophenols are available.

5. Conclusions

Nitrophenols (2-NP, 3-NP, 4-NP, and 2,4-NP) react fast with $SO_4^{\bullet-}$ radical-anions in aqueous solutions. Rate constants for these reactions, along with rate constants of several chlorophenols and phenol, correlate linearly with Brown substituent coefficients and with the relative strength of the O–H bonds in the molecules. The correlation allows estimation of rate constants for reactions of other substituted phenols with sulfate radical-anions.

The aqueous-phase reaction of 2-NP with sulfate radical-anions dominates over the aqueous-phase conversion of 2-NP by OH radicals only when $SO_4^{\bullet-}$ radicals are at least 10 times more abundant than the OH radicals. Similar domination over NO_3 radical requires the concentration of sulfate radicals is at least a quarter of the concentration of nitrate radicals.

The comparison of gas-phase conversion of 2-NP by OH or NO_3 radicals against the aqueous-phase conversion by sulfate radical-anions depends on the liquid water contents of a particular atmospheric system considered. In deliquescent aerosol and haze water ($\omega < 10^{-10}$ m^3 m^{-3}), gas-phase reactions always prevail over the aqueous-phase reactions. In cloud, rain and fog water ($10^{-8} < \omega < 10^{-6}$ m^3 m^{-3}), the aqueous-phase reaction of 2-NP dominates over the gas-phase conversion of 2-NP by hydroxyl or nitrate radicals provided the aqueous-phase concentration of sulfate radical-anions is not smaller than the aqueous-phase concentration of hydroxyl or nitrate radicals. These conclusions are based on the assumption that the gas-phase and aqueous-phase concentrations of OH, NO_3, and 2-NP are bound by Henry's equilibria.

The gas-phase and aqueous-phase conversions of other nitrophenols are expected to follow similar patterns. However, this expectation should be confirmed by calculations when constants of the gas-phase reactions of the nitrophenols with hydroxyl and nitrate radicals are available.

Last not least, we hope that the rate constants determined in the present work for atmospheric purposes may appear useful for designers of advanced oxidation processes aimed at removal of nitrophenols from various waste effluents utilizing sulfate radical-anions.

Supplementary Materials: The following are available online at http://www.mdpi.com/2073-4433/10/12/795/s1, Table S1: Chain mechanism of SIV autoxidation catalyzed by FeIII, Figure S1: Concentration of oxygen recorded during autoxidation of $NaHSO_3$ solution in the presence of nitrophenols, Figure S2: Linear plots of reciprocal quasi-stationary rates for autoxidation of S(IV) in the presence of nitrophenols, Table S2: Properties of nitrophenols and sulfate radical anion, Figure S3: The ratio of the gas-phase and the aqueous-phase conversions of 2-NP by OH and NO_3 radicals.

Author Contributions: Conceptualization, methodology, investigation: K.J.R.; Data curation: K.J.R. and R.S.; Writing—original draft preparation: K.J.R.; Writing—review and editing: K.J.R. and R.S.

Funding: This research received no external funding.

Acknowledgments: The authors are grateful to Irena Grgić for the invitation to contribute to the Special Issue "Atmospheric Aqueous-Phase Chemistry" and to Józef Ziajka for extensive support in the experimental work behind this presentation.

Conflicts of Interest: The authors declare no conflict of interest.

References

1. Harrison, M.A.J.; Barra, S.; Borghesi, D.; Vione, D.; Arsene, C.; Iulian Olariu, R. Nitrated phenols in the atmosphere: A review. *Atmos. Environ.* **2005**, *39*, 231–248. [CrossRef]
2. Michałowicz, J.; Duda, W. Phenols—Sources and Toxicity. *Pol. J. Environ. Stud.* **2007**, *16*, 347–362.
3. Belloli, R.; Bolzacchini, E.; Clerici, L.; Rindone, B.; Sesana, G.; Librando, V. Nitrophenols in air and rainwater. *Environ. Eng. Sci.* **2006**, *23*, 405–415. [CrossRef]
4. Delhomme, O.; Morville, S.; Millet, M. Seasonal and diurnal variations of atmospheric concentrations of phenols and nitrophenols measured in the Strasbourg area, France. *Atmos. Pollut. Res.* **2010**, *1*, 16–22. [CrossRef]
5. Morville, S.; Scheyer, A.; Mirabel, P.; Millet, M. A multiresidue method for the analysis of phenols and nitrophenols in the atmosphere. *J. Environ. Monit.* **2004**, *6*, 963–966. [CrossRef]
6. Morville, S.; Scheyer, A.; Mirabel, P.; Millet, M. Spatial and geographical variations of urban, suburban and rural atmospheric concentrations of phenols and nitrophenols. *Environ. Sci. Pollut. Res.* **2006**, *13*, 83–89. [CrossRef]
7. Huston, R.; Chan, Y.C.; Gardner, T.; Shaw, G.; Chapman, H. Characterisation of atmospheric deposition as a source of contaminants in urban rainwater tanks. *Water Res.* **2009**, *43*, 1630–1640. [CrossRef]
8. Jaber, F.; Schummer, C.; Al Chami, J.; Mirabel, P.; Millet, M. Solid-phase microextraction and gas chromatography—Mass spectrometry for analysis of phenols and nitrophenols in rainwater, as their t-butyldimethylsilyl derivatives. *Anal. Bioanal. Chem.* **2007**, *387*, 2527–2535. [CrossRef]
9. Asman, W.A.H.; Jørgensen, A.; Bossi, R.; Vejrup, K.V.; Bügel Mogensen, B.; Glasius, M. Wet deposition of pesticides and nitrophenols at two sites in Denmark: Measurements and contributions from regional sources. *Chemosphere* **2005**, *59*, 1023–1031. [CrossRef]
10. Hofmann, D.; Hartmann, F.; Herrmann, H. Analysis of nitrophenols in cloud water with a miniaturized light-phase rotary perforator and HPLC-MS. *Anal. Bioanal. Chem.* **2008**, *391*, 161–169. [CrossRef]
11. Boris, A.J.; Lee, T.; Park, T.; Choi, J.; Seo, S.J.; Collett, J.L., Jr. Fog composition at Baengnyeong Island in the eastern Yellow Sea: Detecting markers of aqueous atmospheric oxidations. *Atmos. Chem. Phys.* **2016**, *16*, 437–453. [CrossRef]
12. Chow, K.S.; Huang, X.H.H.; Yu, J.Z. Quantification of nitroaromatic compounds in atmospheric fine particulate matter in Hong Kong over 3 years: Field measurement evidence for secondary formation derived from biomass burning emissions. *Environ. Chem.* **2016**, *13*, 665–673. [CrossRef]
13. Duong, H.T.; Kadokami, K.; Trinh, H.T.; Phan, T.Q.; Le, G.T.; Nguyen, D.T.; Nguyen, T.T.; Nguyen, D.T. Target screening analysis of 970 semi-volatile organic compounds adsorbed on atmospheric particulate matter in Hanoi, Vietnam. *Chemosphere* **2019**, *219*, 784–795. [CrossRef] [PubMed]
14. Fleming, L.T.; Lin, P.; Laskin, A.; Laskin, J.; Weltman, R.; Edwards, R.D.; Arora, N.K.; Yadav, A.; Meinardi, S.; Blake, D.R.; et al. Molecular composition of particulate matter emissions from dung and brushwood burning household cookstoves in Haryana, India. *Atmos. Chem. Phys.* **2018**, *18*, 2461–2480. [CrossRef]
15. Giorio, C.; Bortolini, C.; Kourtchev, I.; Tapparo, A.; Bogialli, S.; Kalberer, M. Direct target and non-target analysis of urban aerosol sample extracts using atmospheric pressure photoionisation high-resolution mass spectrometry. *Chemosphere* **2019**, *224*, 786–795. [CrossRef] [PubMed]

16. Irei, S.; Stupak, J.; Gong, X.; Chan, T.-W.; Cox, M.; McLaren, R.; Rudolph, J. Molecular marker study of particulate organic matter in Southern Ontario air. *J. Anal. Methods Chem.* **2017**, *2017*, 19. [CrossRef] [PubMed]
17. Kitanovski, Z.; Grgic, I.; Vermeylen, R.; Claeys, M.; Maenhaut, W. Liquid chromatography tandem mass spectrometry method for characterization of monoaromatic nitro-compounds in atmospheric particulate matter. *J. Chromatogr. A* **2012**, *1268*, 35–43. [CrossRef]
18. Kitanovski, Z.; Shahpoury, P.; Samara, C.; Voliotis, A.; Lammel, G. Composition and mass size distribution of nitrated and oxygenated aromatic compounds in ambient particulate matter from southern and central Europe—implications for origin. *Atmos. Chem. Phys. Discuss.* **2019**, *2019*, 1–29. [CrossRef]
19. Krivácsy, Z.; Gelencsér, A.; Kiss, G.; Mészáros, E.; Molnár, Á.; Hoffer, A.; Mészáros, T.; Sárvári, Z.; Temesi, D.; Varga, B.; et al. Study on the chemical character of water soluble organic compounds in fine atmospheric aerosol at the Jungfraujoch. *J. Atmos. Chem.* **2001**, *39*, 235–259. [CrossRef]
20. Li, X.; Jiang, L.; Hoa, L.P.; Lyu, Y.; Xu, T.; Yang, X.; Iinuma, Y.; Chen, J.; Herrmann, H. Size distribution of particle-phase sugar and nitrophenol tracers during severe urban haze episodes in Shanghai. *Atmos. Environ.* **2016**, *145*, 115–127. [CrossRef]
21. OÖzel, M.Z.; Hamilton, J.F.; Lewis, A.C. New sensitive and quantitative analysis method for organic nitrogen compounds in urban aerosol samples. *Environ. Sci. Technol.* **2011**, *45*, 1497–1505. [CrossRef] [PubMed]
22. Teich, M.; Pinxteren, D.; Herrmann, H. Determination of nitrophenolic compounds from atmospheric particles using hollow-fiber liquid-phase microextraction and capillary electrophoresis/mass spectrometry analysis. *Electrophoresis* **2014**, *35*, 1353–1361. [CrossRef] [PubMed]
23. Wang, L.; Wang, X.; Gu, R.; Wang, H.; Yao, L.; Wen, L.; Zhu, F.; Wang, W.; Xue, L.; Yang, L.; et al. Observations of fine particulate nitrated phenols in four sites in northern China: Concentrations, source apportionment, and secondary formation. *Atmos. Chem. Phys.* **2018**, *18*, 4349–4359. [CrossRef]
24. Williams, B.J.; Goldstein, A.H.; Kreisberg, N.M.; Hering, S.V.; Worsnop, D.R.; Ulbrich, I.M.; Docherty, K.S.; Jimenez, J.L. Major components of atmospheric organic aerosol in southern California as determined by hourly measurements of source marker compounds. *Atmos. Chem. Phys.* **2010**, *10*, 11577–11603. [CrossRef]
25. Zhang, Y.Y.; Müller, L.; Winterhalter, R.; Moortgat, G.K.; Hoffmann, T.; Pöschl, U. Seasonal cycle and temperature dependence of pinene oxidation products, dicarboxylic acids and nitrophenols in fine and coarse air particulate matter. *Atmos. Chem. Phys.* **2010**, *10*, 7859–7873. [CrossRef]
26. Kristanti, R.A.; Kanbe, M.; Toyama, T.; Tanaka, Y.; Tang, Y.; Wu, X.; Mori, K. Accelerated biodegradation of nitrophenols in the rhizosphere of Spirodela polyrrhiza. *J. Environ. Sci.* **2012**, *24*, 800–807. [CrossRef]
27. Vozňáková, Z.; Podehradská, J.; Kohličková, M. Determination of nitrophenols in soil. *Chemosphere* **1996**, *33*, 285–291. [CrossRef]
28. Chiron, S.; Minero, C.; Vione, D. Occurrence of 2,4-dichlorophenol and of 2,4-dichloro-6-nitrophenol in the Rhone River Delta (Southern France). *Environ. Sci. Technol.* **2007**, *41*, 3127–3133. [CrossRef]
29. Cho, E.; Khim, J.; Chung, S.; Seo, D.; Son, Y. Occurrence of micropollutants in four major rivers in Korea. *Sci. Total Environ.* **2014**, *491–492*, 138–147. [CrossRef]
30. Musilová, J.; Barek, J.; Pecková, K. Determination of nitrophenols in drinking and river water by differential pulse voltammetry at boron-doped diamond film electrode. *Electroanalysis* **2011**, *23*, 1236–1244. [CrossRef]
31. Schmidt-Bäumler, K.; Heberer, T.; Stan, H.-J. Occurrence and distribution of organic contaminants in the aquatic system in Berlin.Part II: Substituted phenols in Berlin surface water. *Acta Hydroch. Hydrob.* **1999**, *27*, 143–149. [CrossRef]
32. Balasubramanian, P.; Balamurugan, T.S.T.; Chen, S.-M.; Chen, T.-W. Simplistic synthesis of ultrafine CoMnO3 nanosheets: An excellent electrocatalyst for highly sensitive detection of toxic 4-nitrophenol in environmental water samples. *J. Hazard. Mater.* **2018**. [CrossRef]
33. Jay, K.; Stieglitz, L. Identification and quantification of volatile organic components in emissions of waste incineration plants. *Chemosphere* **1995**, *30*, 1249–1260. [CrossRef]
34. Goi, A.; Trapido, M. Comparison of advanced oxidation processes for the destruction of 2,4-dinitrophenol. *Proc. Est. Acad. Sci. Chem.* **2001**, *50*, 5–17.
35. Inomata, S.; Fushimi, A.; Sato, K.; Fujitani, Y.; Yamada, H. 4-Nitrophenol, 1-nitropyrene, and 9-nitroanthracene emissions in exhaust particles from diesel vehicles with different exhaust gas treatments. *Atmos. Environ.* **2015**, *110*, 93–102. [CrossRef]

36. Lu, C.; Wang, X.; Dong, S.; Zhang, J.; Li, J.; Zhao, Y.; Liang, Y.; Xue, L.; Xie, H.; Zhang, Q.; et al. Emissions of fine particulate nitrated phenols from various on-road vehicles in China. *Environ. Res.* **2019**, *179*, 108709. [CrossRef] [PubMed]
37. Rubio, M.A.; Bustamante, P.; Vásquez, P. Atmospheric phenolic derivatives as tracers in an urban area. *J. Chil. Chem. Soc.* **2019**, *64*, 4407–4411. [CrossRef]
38. Environmental Protection Agency. *Interim Reregistration Eligibility Decision for Methyl Parathion, Case No. 0153*; Office of Prevention, Pesticides and Toxic Substances, Ed.; United States Environmental Protection Agency: Washington, DC, USA, 2006; p. 20460.
39. World Health Organization. *Parathion in Drinking-Water*; Background document for development of WHO guidelines for drinking-water quality; World Health Organization: Geneva, Switzerland, 2004.
40. Bluvshtein, N.; Lin, P.; Flores, J.M.; Segev, L.; Mazar, Y.; Tas, E.; Snider, G.; Weagle, C.; Brown, S.S.; Laskin, A.; et al. Broadband optical properties of biomass-burning aerosol and identification of brown carbon chromophores. *J. Geophys. Res. Atmos.* **2017**, *122*, 5441–5456. [CrossRef]
41. Priestley, M.; Le Breton, M.; Bannan, T.J.; Leather, K.E.; Bacak, A.; Reyes-Villegas, E.; De Vocht, F.; Shallcross, B.M.A.; Brazier, T.; Anwar Khan, M.; et al. Observations of Isocyanate, Amide, Nitrate, and Nitro Compounds From an Anthropogenic Biomass Burning Event Using a ToF-CIMS. *J. Geophys. Res. Atmos.* **2018**, *123*, 7687–7704. [CrossRef]
42. Xie, M.; Chen, X.; Hays, M.D.; Holder, A.L. Composition and light absorption of N-containing aromatic compounds in organic aerosols from laboratory biomass burning. *Atmos. Chem. Phys.* **2019**, *19*, 2899–2915. [CrossRef]
43. Wang, X.; Gu, R.; Wang, L.; Xu, W.; Zhang, Y.; Chen, B.; Li, W.; Xue, L.; Chen, J.; Wang, W. Emissions of fine particulate nitrated phenols from the burning of five common types of biomass. *Environ. Pollut.* **2017**, *230*, 405–412. [CrossRef] [PubMed]
44. Hinrichs, R.Z.; Buczek, P.; Trivedi, J.J. Solar Absorption by Aerosol-Bound Nitrophenols Compared to Aqueous and Gaseous Nitrophenols. *Environ. Sci.Technol.* **2016**, *50*, 5661–5667. [CrossRef] [PubMed]
45. Lin, P.; Bluvshtein, N.; Rudich, Y.; Nizkorodov, S.A.; Laskin, J.; Laskin, A. Molecular Chemistry of Atmospheric Brown Carbon Inferred from a Nationwide Biomass Burning Event. *Environ. Sci.Technol.* **2017**, *51*, 11561–11570. [CrossRef] [PubMed]
46. Barzaghi, P.; Herrmann, H. A mechanistic study of the oxidation of phenol by OH/NO_2/NO_3 in aqueous solution. *Phys. Chem. Chem. Phys.* **2002**, *4*, 3669–3675. [CrossRef]
47. Heal, M.R.; Harrison, M.A.J.; Neil Cape, J. Aqueous-phase nitration of phenol by N_2O_5 and $ClNO_2$. *Atmos. Environ.* **2007**, *41*, 3515–3520. [CrossRef]
48. Vione, D.; Maurino, V.; Minero, C.; Pelizzetti, E. Aqueous atmospheric chemistry: Formation of 2,4-dinitrophenol upon nitration of 2-nitrophenol and 4-nitrophenol in solution. *Environ. Sci. Technol.* **2005**, *39*, 7921–7931. [CrossRef]
49. Vione, D.; Maurino, V.; Minero, C.; Pelizzetti, E.; Harrison, M.A.J.; Olariu, R.; Arsene, C. Photochemical reactions in the tropospheric aqueous phase and on particulate matter. *Chem. Soc. Rev.* **2006**, *35*, 441–453. [CrossRef]
50. Yuan, B.; Liggio, J.; Wentzell, J.; Li, S.M.; Stark, H.; Roberts, J.M.; Gilman, J.; Lerner, B.; Warneke, C.; Li, R.; et al. Secondary formation of nitrated phenols: Insights from observations during the Uintah Basin Winter Ozone Study (UBWOS) 2014. *Atmos. Chem. Phys.* **2016**, *16*, 2139–2153. [CrossRef]
51. Atkinson, R. Gas-phase tropospheric chemistry of organic compounds. *J. Phys. Chem. Ref. Data Monogr.* **1994**, Monoghraph No. 2, 1–216.
52. Atkinson, R.; Aschmann, S.M.; Arey, J. Reactions of hydroxyl and nitrogen trioxide radicals with phenol, cresols, and 2-nitrophenol at 296 ± 2 K. *Environ. Sci.Technol.* **1992**, *26*, 1397–1403. [CrossRef]
53. Barsotti, F.; Bartels-Rausch, T.; De Laurentiis, E.; Ammann, M.; Brigante, M.; Mailhot, G.; Maurino, V.; Minero, C.; Vione, D. Photochemical Formation of Nitrite and Nitrous Acid (HONO) upon Irradiation of Nitrophenols in Aqueous Solution and in Viscous Secondary Organic Aerosol Proxy. *Environ. Sci.Technol.* **2017**, *51*, 7486–7495. [CrossRef] [PubMed]
54. Vione, D.; Maurino, V.; Minero, C.; Duncianu, M.; Olariu, R.-I.; Arsene, C.; Sarakha, M.; Mailhot, G. Assessing the transformation kinetics of 2-and 4-nitrophenol in the atmospheric aqueous phase. Implications for the distribution of both nitroisomers in the atmosphere. *Atmos. Environ.* **2009**, *43*, 2321–2327. [CrossRef]

55. Hems, R.F.; Abbatt, J.P.D. Aqueous Phase Photo-oxidation of Brown Carbon Nitrophenols: Reaction Kinetics, Mechanism, and Evolution of Light Absorption. *ACS Earth Space Chem.* **2018**, *2*, 225–234. [CrossRef]
56. Li, Y.J.; Huang, D.D.; Cheung, H.Y.; Lee, A.K.Y.; Chan, C.K. Aqueous-phase photochemical oxidation and direct photolysis of vanillin—A model compound of methoxy phenols from biomass burning. *Atmos. Chem. Phys.* **2014**, *14*, 2871–2885. [CrossRef]
57. Wei, B.; Sun, J.; Mei, Q.; He, M. Mechanism and kinetic of nitrate radical-initiated atmospheric reactions of guaiacol (2-methoxyphenol). *Comp. Theor. Chem.* **2018**, *1129*, 1–8. [CrossRef]
58. Yu, L.; Smith, J.; Laskin, A.; Anastasio, C.; Laskin, J.; Zhang, Q. Chemical characterization of SOA formed from aqueous-phase reactions of phenols with the triplet excited state of carbonyl and hydroxyl radical. *Atmos. Chem. Phys.* **2014**, *14*, 13801–13816. [CrossRef]
59. Yu, L.; Smith, J.; Laskin, A.; George, K.M.; Anastasio, C.; Laskin, J.; Dillner, A.M.; Zhang, Q. Molecular transformations of phenolic SOA during photochemical aging in the aqueous phase: Competition among oligomerization, functionalization, and fragmentation. *Atmos. Chem. Phys.* **2016**, *16*, 4511–4527. [CrossRef]
60. Litter, M.I. Introduction to Photochemical Advanced Oxidation Processes for Water Treatment. In *Environmental Photochemistry Part II*; Boule, P., Bahnemann, D.W., Robertson, P.K.J., Eds.; Springer: Berlin/Heidelberg, Germany, 2005; Volume 2, Pt M, pp. 325–366.
61. Goi, A.; Trapido, M. Hydrogen peroxide photolysis, Fenton reagent and photo-Fenton for the degradation of nitrophenols: A comparative study. *Chemosphere* **2002**, *46*, 913–922. [CrossRef]
62. Ahn, W.-Y.; Sheeley, S.A.; Rajh, T.; Cropek, D.M. Photocatalytic reduction of 4-nitrophenol with arginine-modified titanium dioxide nanoparticles. *Appl. Catal. B Environ.* **2007**, *74*, 103–110. [CrossRef]
63. Ali, I.; Hassan, A.; Shabaan, S.; El-Nasser, K. Synthesis and characterization of composite catalysts Cr/ZSM-5 and their effects toward photocatalytic degradation of p-nitrophenol. *Arab. J. Chem.* **2017**, *10*, S2106–S2114. [CrossRef]
64. Priya, M.H.; Madras, G. Kinetics of photocatalytic degradation of chlorophenol, nitrophenol, and their mixtures. *Ind. Eng. Chem. Res.* **2006**, *45*, 482–486. [CrossRef]
65. Liu, Y.; Liu, H.; Li, Y. Comparative study of the electrocatalytic oxidation and mechanism of nitrophenols at Bi-doped lead dioxide anodes. *Appl. Catal. B Environ.* **2008**, *84*, 297–302. [CrossRef]
66. Christensen, P.A.; Egerton, T.A.; Kosa, S.A.M.; Tinlin, J.R.; Scott, K. The photoelectrocatalytic oxidation of aqueous nitrophenol using a novel reactor. *J. Appl. Electrochem.* **2005**, *35*, 683–692. [CrossRef]
67. Zhou, M.; Lei, L. An improved UV/Fe^{3+} process by combination with electrocatalysis for p-nitrophenol degradation. *Chemosphere* **2006**, *63*, 1032–1040. [CrossRef] [PubMed]
68. Apolinário, Â.C.; Silva, A.M.T.; Machado, B.F.; Gomes, H.T.; Araújo, P.P.; Figueiredo, J.L.; Faria, J.L. Wet air oxidation of nitro-aromatic compounds: Reactivity on single-and multi-component systems and surface chemistry studies with a carbon xerogel. *Appl. Catal. B Environ.* **2008**, *84*, 75–86. [CrossRef]
69. Diaz, E.; Polo, A.M.; Mohedano, A.F.; Casas, J.A.; Rodriguez, J.J. On the biodegradability of nitrophenols and their reaction products by catalytic hydrogenation. *J. Chem. Technol. Biotechnol.* **2012**, *87*, 1263–1269. [CrossRef]
70. Anipsitakis, G.P.; Dionysiou, D.D.; Gonzalez, M.A. Cobalt-Mediated Activation of Peroxymonosulfate and Sulfate Radical Attack on Phenolic Compounds. Implications of Chloride Ions. *Environ. Sci. Technol.* **2006**, *40*, 1000–1007. [CrossRef]
71. EPA. The Original List of Hazardous Air Pollutants. Available online: http://www.epa.gov/ttn/atw/188polls.html (accessed on 29 October 2014).
72. EPA. Priority Pollutants. Available online: http://water.epa.gov/scitech/methods/cwa/pollutants.cfm (accessed on 27 October 2014).
73. Keith, L.; Telliard, W. ES&T Special Report: Priority pollutants: I-a perspective view. *Environ. Sci.Technol.* **1979**, *13*, 416–423. [CrossRef]
74. Gramatica, P.; Santagostino, A.; Bolzacchini, E.; Rindone, B. Atmospheric monitoring, toxicology and QSAR modelling of nitrophenols. *Fresenius Environ. Bull.* **2002**, *11*, 757–762.
75. Schafer, K.S.; Reeves, M.; Spitzer, S.; Kegley, S.E. *Chemical Trespass Pesticides in our Bodies and Corporate Accountability*; Pesticide Action Network North America: San Francisco, CA, USA, 2004.
76. Zhang, D.-P.; Wu, W.-L.; Long, H.-Y.; Liu, Y.-C.; Yang, Z.-S. Voltammetric Behavior of o-Nitrophenol and Damage to DNA. *Int. J. Mol. Sci.* **2008**, *9*, 316–326. [CrossRef]

77. Buxton, G.V.; Salmon, G.A.; Williams, J.E. The reactivity of biogenic monoterpenes towards OH·and SO_4^- radicals in de-oxygenated acidic solution. *J. Atmos. Chem.* **2000**, *36*, 111–134. [CrossRef]
78. Clifton, C.L.; Huie, R.E. Rate constants for hydrogen abstraction reactions of the sulfate radical, SO_4^-. Alcohols. *Int. J. Chem. Kinet.* **1989**, *21*, 677–687. [CrossRef]
79. George, C.; Rassy, H.E.; Chovelon, J.M. Reactivity of selected volatile organic compounds (VOCs) toward the sulfate radical (SO_4^-). *Int. J. Chem. Kinet.* **2001**, *33*, 539–547. [CrossRef]
80. Herrmann, H.; Hoffmann, D.; Schaefer, T.; Bräuer, P.; Tilgner, A. Tropospheric Aqueous-Phase Free-Radical Chemistry: Radical Sources, Spectra, Reaction Kinetics and Prediction Tools. *ChemPhysChem* **2010**, *11*, 3796–3822. [CrossRef] [PubMed]
81. Rudzinski, K.J. Degradation of Isoprene in the Presence of Sulphoxy Radical Anions. *J. Atmos. Chem.* **2004**, *48*, 191–216. [CrossRef]
82. Rudziński, K.J.; Gmachowski, L.; Kuznietsova, I. Reactions of isoprene and sulphoxy radical-anions—A possible source of atmospheric organosulphites and organosulphates. *Atmos. Chem. Phys.* **2009**, *9*, 2129–2140. [CrossRef]
83. Ziajka, J.; Rudzinski, K. Autoxidation of S-IV inhibited by chlorophenols reacting with sulfate radicals. *Environ. Chem.* **2007**, *4*, 355–363. [CrossRef]
84. Ziajka, J.; Pasiuk-Bronikowska, W. Autoxidation of sulphur dioxide in the presence of alcohols under conditions related to the tropospheric aqueous phase. *Atmos. Environ.* **2003**, *37*, 3913–3922. [CrossRef]
85. Ziajka, J.; Pasiuk-Bronikowska, W. Rate constants for atmospheric trace organics scavenging SO_4^- in the Fe-catalysed autoxidation of S(IV). *Atmos. Environ.* **2005**, *39*, 1431–1438. [CrossRef]
86. Grgić, I.; Podkrajšek, B.; Barzaghi, P.; Herrmann, H. Scavenging of SO_4^- radical anions by mono-and dicarboxylic acids in the Mn(II)-catalyzed S(IV) oxidation in aqueous solution. *Atmos. Environ.* **2007**, *41*, 9187–9194. [CrossRef]
87. Elliot, A.J.; McCracken, D.R.; Buxton, G.V.; Wood, N.D. Estimation of rate constants for near-diffusion-controlled reactions in water at high temperatures. *J. Chem. Soc. Faraday Trans.* **1990**, *86*, 1539–1547. [CrossRef]
88. Zhu, L.; Nicovich, J.M.; Wine, P.H. Temperature-dependent kinetics studies of aqueous phase reactions of SO_4^- radicals with dimethylsulfoxide, dimethylsulfone, and methanesulfonate. *J. Photochem. Photobiol. A* **2003**, *157*, 311–319. [CrossRef]
89. Noyes, R.M. Effects of diffusion rates on chemical kinetics. In *Progress in Reaction Kinetics*; Porter, G., Stevens, B., Eds.; Pergamon Press: Oxford, UK, 1961; Volume 1, pp. 129–160.
90. North, A.M. *The Collision Theory of Chemical Reactions in Liquids*; Methuen: London, UK, 1964.
91. Hansch, C.; Leo, A.; Taft, R.W. A survey of Hammett substituent constants and resonance and field parameters. *Chem. Rev.* **1991**, *91*, 165–195. [CrossRef]
92. Jones, R.A.Y. *Physical and Mechanistic Organic Chemistry;* Cambridge University Press: Cambridge, MA, USA, 1979.
93. Jonsson, M.; Lind, J.; Eriksen, T.E.; Merényi, G. O–H bond strengths and one-electron reduction potentials of multisubstituted phenols and phenoxyl radicals. Predictions using free energy relationships. *J. Chem. Soc. Perkin Trans. 2* **1993**, 1567–1568. [CrossRef]
94. Herrmann, H.; Schaefer, T.; Tilgner, A.; Styler, S.A.; Weller, C.; Teich, M.; Otto, T. Tropospheric aqueous-phase chemistry: Kinetics, mechanisms, and its coupling to a changing gas phase. *Chem. Rev.* **2015**, *115*, 4259–4334. [CrossRef]
95. Atkinson, R. Kinetics and mechanisms of the gas-phase reactions of the hydroxyl radical with organic compounds. *Chem. Ref.* **1989**, Monograph No. 1. 1–246.
96. Herrmann, H. Kinetics of Aqueous Phase Reactions Relevant for Atmospheric Chemistry. *Chem. Rev.* **2003**, *103*, 4691–4716. [CrossRef]
97. Guo, X.X.; Brimblecombe, P. Henry's law constants of phenol and mononitrophenols in water and aqueous sulfuric acid. *Chemosphere* **2007**, *68*, 436–444. [CrossRef]